Cairo University

Faculty of Science

Physics Department

Thermodynamics of Nuclear Matter at High Energy Nuclear Reactions

Presented by

Zeinab Abdelhalim Abdelrazik

A thesis submitted

To

Faculty of Science

In partial fulfilment of the

Requirements for the degree of

Master of Science.

(Theoretical physics)

Department of physics,

Faculty of Science,

Cairo university.

(2023)

Acknowledgement

Thanks, God, for helping me.

I express my gratefulness to my family for their support and love. Furthermore, I would like to give my appreciation to Prof.Mohamed Tarek Hussein and Prof. Mohamed Tawfik Ghoneim in the Physics Department, Faculty of Science, Cairo University. They have been a great source of knowledge and encouragement and gave me great support and valuable guidance along the course of my thesis. I would like to express my gratitude to them for their significant help during this work.

Abstract

The ultimate goal of the thesis is to study the variations in states of nuclear matter under extreme conditions of pressure, density, and temperature that result from nuclear reactions with high interaction energy. Utilising the experimental quantities, such as; multiplicity, transverse momentum, and rapidity distributions of produced charged particles, to follow up on changes in thermodynamic parameters of the nuclear medium. The study covers a wide spectrum of high-energy nuclear reactions, from simple proton-proton interactions to sophisticated systems with heavy ions. The results are analysed using several thermo-statistical models, revealing the thermodynamic parameters such as chemical potential, non-equilibrium index, and temperature at the kinetic freeze-out stage. Accordingly, the phase diagrams are established in terms of extracted thermodynamic parameters. The results guide the simulation of a scenario and script for the time evolution of charged particles production through various proton-proton and heavy ion collisions.

List of Contents

Acknowledgement	I
Abstract	II
List of tables	IV
List of figures	IV
List of Abbreviations	V
Summary	VI
I. Introduction	1
II. Theoretical interaction models	5
II.1. Fireball	5
II.2. Fire-streak	6
II.3. Fermi-landau	7
II.4. Thermalized cylinder	9
II.5. Thermo-statistical	10
III. Experimental Data	18
IV. Results and discussion	19
V. Conclusions	35
References	37

LIST OF TABLES

ID	Table Caption	Page
Table (I)	The values of the kinetic freeze-out temperature T and formation time t_c in p-p collision at 6.3 GeV at different rapidity regions.	21
Table (II)	Parameters from the equivalent Gaussian fit to the pseudo-rapidity distribution of the shower particles emitted in 4.5A GeV/c ^{28}Si-Em Interactions for central, semi-central, semi-peripheral and peripheral.	30
Table (III)	Values of kinetic freeze-out temperature T, average transverse momentum $<p_t>$, the non-equilibrium factor q and the entropy density for central, semi-central, semi-peripheral and peripheral interactions of ^{28}Si-Em at 4.5A GeV/c using Tsallis distribution function.	32

LIST OF FIGURES

ID	Figure Caption	Page
II. Theoretical interaction models		
Fig.(II.1)	Schematic illustrations of nucleus-nucleus collisions viewed by the "Fireball" Model.	5
Fig.(II.2)	Schematic illustrations of nucleus-nucleus collisions viewed by the "Fire-streak" Model.	6
Fig.(II.3)	Schematic illustrations of nucluse-nucluse collision according to the fermi-landau model.	7
IV. Results and discussion		
Fig.(IV.1)	Transverse momentum distribution of the produced hadrons at 6.3 GeV at different rapidity slices.	19
Fig. (IV.2)	The relation between the effective temperature T_{eff} and entropy density σ_s for p-p collisions at ISR interaction energy at central rapidity range (y = 0.0 - 2.0).	21
Fig.(IV.3)	The correlation between the effective temperature T_{eff} and entropy density σ_s of charged hadrons produced in pp collision at $\sqrt{s}$ = 0.9, 2.36 and 7 TeV.	22
Fig. (IV.4)	The chemical potential -temperature (μ-T) phase diagram of particles produced in the final state of p-p collisions at different center of mass energies.	24

Fig. (IV.5)	Variation of the freeze-out temperature with the pseudo-rapidity of produced hadrons through p-p collisions at a different center of mass energies.	25
Fig. (IV.6)	Change of the non-equilibrium parameter q with the temperature T for particles produced in the p-p collision for the GeV energy group and TeV energy group.	26
Fig.(IV.7)	A schematic diagram of the origin of the pseudo-rapidity of the produced particles in heavy ion collisions in the AGS energy region (fig.7-a) and in the RHIC and LHC one (fig.7-b).	27
Fig.(IV.8)	Pseudo-rapidity distribution of the shower particles emitted in 4.5A GeV/c ^{28}Si-Em Interactions for central, semi-central, semi-peripheral and peripheral.	29
Fig.(IV.9)	The change of the non-equilibrium parameter q with the temperature T of the produced particles in heavy ion collisions for GeV (fig.9-a) and TeV group of energy (fig.9-b).	33

List of Abbreviations:

Abbreviation	Definition
AGS	Alternating Gradient Synchrotron.
ALICE	A Large Ion Collider Experiment.
GeV	Giga electron volt, a unit of energy equal to 10^9 electron volts.
ISR	The Intersecting Storage Rings, hadron accelerator.
LHC	Large Hadron Collider.
PDG	particle data group
QCD	Quantum Chromo Dynamics.
QGP	Quark-gluon plasma.
RHIC	Relativistic Heavy Ion Collider.
TeV	Tera electron Volts, a unit of energy equal to 10^{12} electron volts.

SUMMARY

The present work aims to study the possible states of nuclear matter and the location of phase boundaries between hadronic gas and the quark-gluon plasma phase . The boundary at the hadron freeze-out is also considered. Proton-proton collisions at a wide range of center of mass energies are used to examine the phase transition (entropy-temperature) diagram. Local thermodynamic equilibrium is assumed at different intervals of rapidity space. The entropy of the system is expressed in terms of the multiplicity of hadron production in each rapidity interval. However, the local temperature is estimated using the average transverse momentum. The values of the critical temperatures are found at the boundaries of the phases with a quite clear description of the states.

The experimental data of charged particles produced in proton-proton collisions extracted from the Durham particle data group (PDG) at energy ranges $\sqrt{s}$ = 6.3 - 17 GeV and at 0.9 - 7 TeV are investigated in the framework of thermo-statistical models and the Vlasov time dynamics. The analysis is used to describe the experimental data all over the considered energies and rapidity intervals. The variation of the collision parameters (chemical potential, entropy, non-equilibrium factor and the time of evolution) is studied and discussed as a function of the final state temperature. According to the obtained result, a scenario, and a script of the time evolution for the particle production is simulated by the obtained data of the p-p collision.

The need of in-depth study of the nuclear matter when doing scientific research for phase transition, one had to go to the heavy ion collision that offers high energy density that enables studying the fine structure of the nuclear matter up to quark-Gluon Plasma (QGP) state.

Numerous numbers of nuclear reaction experiments at a wide range of energy from few GeV up to few TeV values has been offering a lot of data, including proton-proton, proton-nucleus as well as nucleus-nucleus collisions. The increase in interaction energy at these experiments has been making nuclear matter go through different phases as it is exposed to higher pressure, energy density and temperature. The data that came out from high-energy nuclear reactions have made the possibility to study particle production, the properties of which have led to valuable information about the phase transitions. This study focused on the interactions of p-p and nuclues-nucluse in view of the thermo-statistical approach to detect the variations that take place in the nuclear medium by studying how the rapidity of the produced charged particles, entropy density, non-equilibrium factor and the temperature of the system change as the centrality of the collision changes.

In particular, the study has covered the properties of the produced charged particles through the different Proton-Proton and nucleus-nucleus collisions, such as the transverse momentum spectra of produced charged hadrons through inelastic p-p interactions at the centre of mass energies per nucleon pair equal to 6.3, 7.7, 8.8, 12.3 17.3 GeV at rapidity ranges y from 0.0 to 2.0. Also, the transverse momentum distributions of the produced charged hadrons through proton-proton collision at different energies = 0.9, 2.36, 7 TeV at the mid-rapidity range. While the investigated nucleus-nucleus collisions have been accomplished through analysing the pseudo-rapidity distribution of the shower particles emitted in 4.5 A GeV/c ^{28}Si interactions with the emulsion plate.

In addition, analysing the transverse momentum distributions of the produced charged hadrons through different A-A collisions at different energies in the GeV and TeV regions at the mid-rapidity range. For instance, using the Tsallis distribution function to fit the transverse momentum distribution of produced charged hadrons at mid-rapidity measured for Au-Au collisions at $\sqrt{s_{NN}}$= 19.6 and 62.4 GeV for six centrality classes.

By analyzing the transverse momentum distribution of produced charged particles at low transverse momentum (below 3 GeV/c) and mid-rapidity intervals, where the particles are affected by transverse flow, using statistical thermodynamic models, it was feasible to extract thermodynamic parameters including chemical potential, non-equilibrium factor, and temperature at the kinetic freeze-out stage. Consequently, the phase transition diagrams are more convenient to be in the form of the (entropy-temperature) and the (chemical potential-temperature) diagrams.

CHAPTER (I)
INTRODUCTION

I. INTRODUCTION:

The quantum chromodynamics (QCD) phase diagram [1] contains a variety of theoretically predicted features. The most important one is the phase boundary which separates the hadron gas phase and the quark-gluon plasma phase. Information on the properties of the QCD phase diagram through systematic studies of the system size and the energy dependence of particle production in hadron-hadron and heavy ion collisions are investigated at a wide range of interaction energy. Generally, the phase transition can be examined by following changes in temperature, pressure, entropy… etc. of the system. So, when the nuclear matter goes through high energy collisions it creates high temperatures and high densities like that of the core of the sun (5 - 10 times the density of nuclear matter) [2].

These conditions force the nuclear matter to go through a phase transition and get into the quark-gluon plasma (QGP) phase which still has a mysterious nature. After the expansion of the system, this hot de-confinement state QGP goes through a phase of forming many hadron particles. The high multiplicity of the produced hadron particles generated by the same scenario through the proton-proton collision experiments could be handled by thermal-statistical models. Once the system reaches near thermal equilibrium, one can extract its characteristics by several thermo-dynamical observables such as its volume, temperature, energy density and entropy. The order of phase transition will be studied in view of the thermodynamic picture. The nature of transition can be a genuine phase transition, first-order, or crossover over a small temperature range. The first-order phase transition is characterized by continuous behavior; however, the crossover is a rapid change with temperature. The particle production in the proton-proton collisions will be considered the key player in

detecting the phase transition and getting a sufficient view of the nature of the strong force acting inside the hadron and studying its dependence on the number of quarks flavors and colors. The location of the critical temperature at which the phase transition turns on is still very uncertain. A boundary line separates the normal hadronic phase from another one known as the quarkyonic phase [3,4].

Experimentally, there are several control parameters available that might allow studying different regions of the phase diagram with hadron collisions. One; is the variation of the center-of-mass energy which will force the reaction systems to follow different trajectories in the temperature-chemical potential (T-μ plane), reflected by a change in the chemical freeze-out parameters. The second control parameter is the variation of the system size, which can either be achieved by performing collisions of hadrons (at different impact parameters) of different sizes; or by studying centrality selected minimum bias collisions considering the entropy density versus temperature at different rapidity intervals. This can be considered a good control parameter for probing different areas of the phase diagram and shall be discussed further below. To determine different areas in the QCD phase diagram, the variation of the center-of-mass energy can be considered the best-defined control parameter. In an energy range starting from a few GeV up to the TeV region, a wide region in the entropy-temperature (σ-T) plane can be explored experimentally, as is evident from the strong dependence of the temperature freeze-out parameters on the energy. The trajectories of the fireballs in the core might always be the same, irrespective of their size [5]. So, studying centrality dependences in asymmetric proton-hadron reaction systems could provide an additional experimental test of the production mechanism[6].

In this thesis, the experimental features which point out the existence of the phase transition and its nature are studied by relating the change in the macroscopic

variables such as transverse momentum, and multiplicity distribution to the microscopic hypothesis of the transition mechanism.

The measurable physical quantities of produced particles at high energy are helpful information to recognize the states of phase transition in nuclear matter. In a wide energy range, there are some common aspects of interaction dynamics. However, when Quark-Gluon Plasma is formed, the number of quanta increases to a large extent [1,2] and can reveal much about the physics of particle production. Over the past two decades, numerous experimental collaborations at the RHIC and LHC have collected a wealth of data on the transverse momentum spectra of particles, spanning from p-p collisions through Pb-Pb collisions at various energies and centralities. The study of the experimental data of hadron collisions or heavy ion collisions which are carried out in complex experiments like RHIC and LHC, is not a direct study for extracting the system information. Measurable quantities such as the transverse momentum spectra and the rapidity of the produced particles could provide us with the transverse flow velocity of produced particles, kinetic freeze-out temperature, and volume of the interacting system. These could also indicate the excitation degree of the interacting system [3]. To describe the transverse momentum spectra of the particles, numerous theoretical models have been considered such as the Tsallis statistics which has recognized much attention due to its successful applications to the particle transverse momentum spectra and the pseudo-rapidity distribution of charged particles produced in high energy proton-proton and heavy-ion collisions [7-14]. Particle collisions may contribute to this field at two points: the dynamics of the phase transitions in “small” systems, and the dynamics of the phase transitions in ultra-relativistic systems where the energy of the system is much higher than the rest mass of the produced particles.

This would give a clue to understand the symmetry problem which is important to describe the equation of state inside a thermodynamic nuclear system and may give some information on the natural structure of QCD.

In this study, the interactions of ^{28}Si with emulsion nuclei at 4.5 AGeV/c is investigated in view of thermo-statistical approach to get some information of the variations of physical quantities, stated above, that take place in the nuclear medium and compare them with their corresponding parameters that came out of other nuclear reactions at different energies and masses.

CHAPTER (II)
Theoretical interaction models

II. Theoretical interaction models:

II.1. Fireball model[15]:

This model assumes that nucleus-nucleus reaction could be described by two main steps; at the first, the projectile and target nuclei sequence through each other, forming a cylinder cut as shown in fig.(II.1), creating an overlap region from the target and projectile participants at certain impact parameter. This overlap region forms a quasi-equilibrated system, called “fireball”. Second, after the collision, the overlapping domains (from the projectile and target) melt together and come to rest in the center of the mass of the fireball. In the rest frame of the fireball, the produced particles are emitted isotopically. In the relatively slow stage after the collision, the spectators of both the target and the projectile decay because of the induced excitation by several processes such as re-absorption of pions, compressional energy… etc.

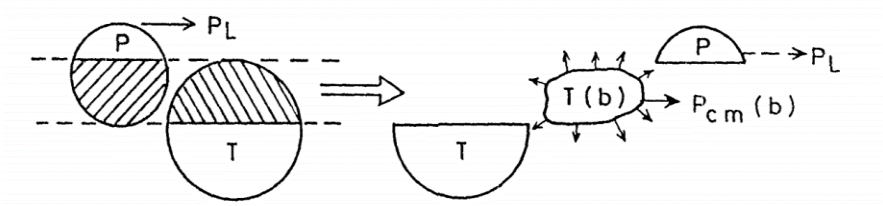

Fig.(II.1): Schematic illustrations of nucleus-nucleus collisions viewed by the “Fireball” Model.

According to the above description, the main power of creating such thermal motion of produced particles in the final channel is the kinetic energy in the initial channel in which the fireball is created. In addition to that, the energy density in the center of the fireball is extremely high so that it could be considered an ideal-relativistic gas. The model is concerned with the fireball evaluation rather than the remains of the spectators.

This model could succeed in reproducing the experimental data of the proton multiplicity and angular distribution at low energies, up to 400 MeV, but it is overestimated at high ranges of energy and in collisions with low-impact parameters.

II.2. Fire-streak model [16]:

This is an extension of the fireball model, as it assumes that the collision components are tiny slices streaks which travel in parallel to the beam axis as shown in fig. (II.2).

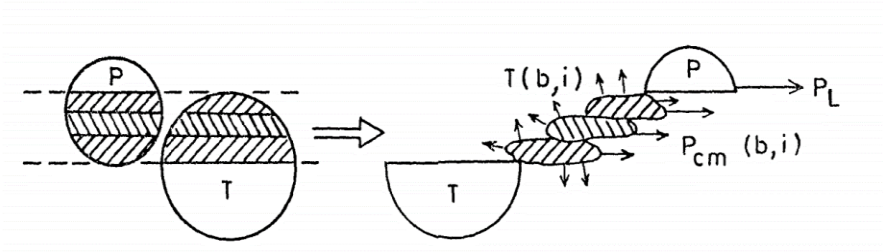

Fig.(II.2): Schematic illustrations of nucleus-nucleus collisions viewed by the "Fire-streak" Model.

During the collision process, the projectile and target streaks collide with each other to start the reaction. This results in small fireballs with a center of mass velocity and temperature that are all dependent on how much matter the projectile streak contributes, which in turn, depends on the impact parameter.

Thus, the kinematics which describes the two-streak collision is like that of the fireball. One might add here that the Fire-streak model assumes a diffused surface of nuclear matter instead of the sharp sphere picture assumed by the fireball one. In fact, this could be more suitable for the production of light composite fragments.

II.3. Fermi-Landau Model[17,18]:

This model assumes that at the beginning of collision, the two ion beams have energies greater than their rest mass, travelling at a speed that approaches that of light. They are made to collide with each other, such that, the two incoming nucleons in heavy-ion collisions due to the Fermi model look like two flying disks toward each other, surrounded by a cloud of pions, as shown in Fig. (II.3). The pion clouds extend to a region of distance in the order of $\hbar c/m_\pi$. The cloud is assumed to have a spherical shape of radius R, given as:

$$R = \frac{\hbar c}{m_\pi} \ldots\ldots \qquad (1)$$

Where $\hbar c$ is the conversion constant, m_π is the pion mass. The collision zone is assumed to take a spherical shape so that the interaction volume can be estimated as follow:

$$V = \frac{4}{3}\pi R^3 \quad \ldots. \qquad (2)$$

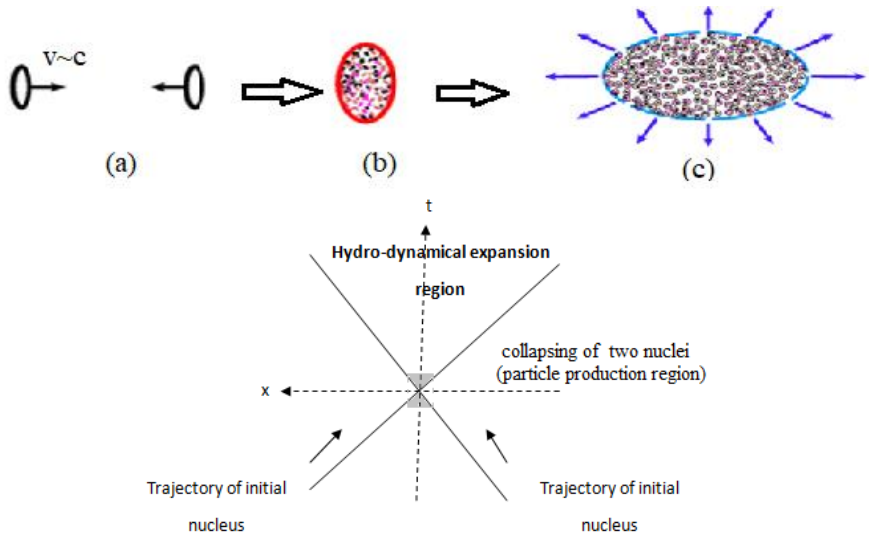

Fig.(II.3): Schematic illustrations of nucluse-nucluse collision according to the fermi-landau model [18,19]; a) two colliding nuclei travelling at the speed of light, b) two nuclei collapsing, c)expansion of hadronic matter and d)time–space diagram of nucleus-nucleus collision.

After a formation time, a volume with high energy density is created. After equilibration, the evolution of a hot QCD matter follows the laws of relativistic hydrodynamics is settled. First, there is a longitudinal expansion until the system reaches a longitudinal size close to its transverse size, and then a tridimensional expansion starts until the density is so low that no more collisions take place. The system reaches then the so-called chemical freeze-out. Finally, all the particles would decay to their daughter particles or reach the detector. Typically, only charged pions, kaons, protons, neutrons, photons, electrons, and muons will reach the detectors.

The available energy in the center of mass is assumed to be dissipated during the collision into the internal degrees of freedom of the nucleus-nucleus system. Under this hypothesis, the energy density of the drop will approximately be given by the macroscopic observables such as the volume, the multiplicity distribution, and the transverse momentum. Therefore, the initial energy density could be deduced in the system of a head-on collision, as [20]:

$$\varepsilon = \frac{\frac{3}{2}\frac{dN_{\mathrm{ch}}}{d\eta} <P_t>}{V} \quad \ldots\ldots \quad (3)$$

Where, V is the volume into which the energy is deposited, $< P_t >$ the average transverse momentum of the produced particles and $\frac{dN_{\mathrm{ch}}}{d\eta}$ is the rapidity density or, the number N_{ch} of produced pions in the rapidity interval $d\eta$. Then, the initial entropy density in the system of a head-on collision could be estimated as:

$$\sigma_s = \frac{\frac{dN_{\mathrm{ch}}}{d\eta}\frac{3}{2}}{s} \quad \ldots\ldots \quad (4)$$

The interaction volume of the overlap region of the two colliding particles depends mainly on the impact parameter.

The interacting cross-section area is denoted by s, which is considered an area of a circle and the values of entropy density are varied due to the estimation of this area. Both the energy density and the random motion increase with the multiplicity per rapidity interval, $\frac{dN_{\mathrm{ch}}}{d\eta}$.

II.4. Thermalized cylinder model[21,22]

This model takes into consideration the one-dimensional string and the fireball model's most basic image. In relativistic nucleon-nucleon collisions, a string is created that has an interior constant energy per unit length and two extremities that serve as energy reservoirs. The string would split into numerous substrings along the direction of the incident beam due to the asymmetry of the mechanism. The width of the pseudo-rapidity distribution will be determined by the substring distribution length. The fireball model postulates that once the incident nucleon passes through the target nucleon, the fire-streak forms along the path of the incident beam. The width of the pseudo-rapidity distribution will depend on how long the fire-streak is. There are numerous strings or fire-streaks created along the incident direction in relativistic nucleus-nucleus collisions. Due to the transverse mixing of these fire-streaks or strings, a thermalized cylinder is formulated. Therefore, it is assumed that the thermalized cylinder created in nucleus-nucleus collisions is in the rapidity range $[y_{min},y_{max}]$ in the laboratory reference frame. In the rapidity space, an emission plane is formed by the emission points in the thermalized cylinder that have the same rapidity,y_x. In general, emission points with the same coordinates have distinct velocities, these emission points are located on various emission planes in the rapidity space. Based on that the particles are isotopically released in the emission plane's rest frame.

In the laboratory reference frame, the pseudo-rapidity distribution of the particles produced in the emission plane with rapidity,y_x is described by:

$$f(\eta, y_x) = \frac{1}{2cosh^2(\eta - y_x)} \approx \frac{1}{\sqrt{2\pi}\,\sigma} e^{-\frac{(\eta - y_x)^2}{2\sigma^2}} \quad \ldots (5)$$

Where $\sigma$is the width of the distribution. The whole thermalized cylinder, as well as the projectile and target spectators, contribute to the measured pseudo-rapidity distribution in the final state. Then, the pseudo-rapidity density could be calculated by taking into account the integral of Eq. (5) as well as the contributions of the leading projectile and target protons in participants and spectators.

II.5. Thermo-statistical models [23-25]

These are some models that describe the collisions of two heavy ions at high energies by assuming that; a heated system of generated particles and nucleons that extends from an initial state to a break-up state where interactions end. During the expansion, there are several dynamical processes that occur through which fragmented nuclei are formed and different particles are produced. The interaction continues until the mean free paths describing the various dynamical processes are approaching the size of the system. After that, the system becomes non-interacting, and it is considered that the multiplicity of the different species at the break-up stage reflects an equilibrium at the freeze-out stage. According to Van't Hoff reaction box, the phase space distribution of produced particles is considered quasi-classical. The model's predictions could be useful for figuring out the influence of viscosity in heavy ion collisions.

The first step in describing such multiple formation processes was Fermi's attempt in which he suggested the usage of statistical techniques in analyzing the

numerous productions of particles. Then, because of the strong interactions that exist between these particles, the distribution of the energy and the number of produced particles may be governed by statistical tools rather than by any specific theory of the detailed dynamics of the process. When the thermal equilibrium is reached, the system can be characterized by thermo-dynamical observables, such as volume, temperature, energy density and entropy density. Phase transitions of nuclear matter have been studied in view of this model by investigating some experimental physical quantities, as would be introduced in the following sections:

(i) In order to find out the reliability of the collected data using the thermo-statistical aspects which are typically used for systems with particles in local thermodynamic equilibrium as occurs in heavy ion collisions[26]: There are three distinguished statistical ensembles; micro-canonical, canonical and grand-canonical, but the system of relativistic heavy ion collision could be described by a grand canonical ensemble because the volume and chemical potential are consistent at the final state. So, the probability to find a particle at a given energy level j is given by:

$$P_j = \frac{e^{-\frac{E_j}{K_B T}}}{Z} \quad \ldots. \quad (6)$$

Where, Z is the grand-canonical partition function for a relativistic ideal quantum gas of hadrons particle type, then all other thermodynamic quantities could be calculated by the same method.

The ultra-relativistic heavy ion collision experiments produce the events of the high multiplicity of particles so they can be treated by thermal-statistical models. Practically, the average transverse momentum is calculated at each rapidity interval considered as local equilibrium.

Based on that; the transverse momentum distribution could be described by exponential distribution as follows [27]:

$$f(P_t) = \frac{1}{P_t}\frac{dN}{dP_t} \approx A\, e^{-\frac{P_t}{T_{eff}}} \quad \ldots\ldots \quad (7)$$

Where A is the normalization factor while T_{eff} is the effective local temperature of the system which is smaller than the initial temperature because of the longitudinal cooling [31].T_{eff}can be estimated using the average value of the transverse momentum for the finite range of P_t as following [28-30]:

$$< P_t > = \frac{\int_a^b P_t\ dP_t\ P_t\ f(P_t)}{\int_a^b dP_t\ P_t\ f(P_t)} \quad \ldots\ldots \quad (8)$$

$$< P_t > = \ 2\,T_{eff} + \frac{a^2 e^{-\frac{a}{T_{eff}}} - b^2 e^{-\frac{b}{T_{eff}}}}{(a+T_{eff})e^{-\frac{a}{T_{eff}}} - (b+T_{eff})e^{-\frac{b}{T_{eff}}}} \quad \ldots. \quad (9)$$

The effective temperature T_{eff} is estimated by solving the above equation as a function of the average transverse momentum for each rapidity interval. The rapidity of the produced particles would reflect the different local equilibrium regions.

There are three types of temperatures: initial temperature, chemical freeze-out temperature, and kinetic freeze-out temperature, which describe the excitation degrees of an interacting system at the stages of initial collisions. An effective temperature is a form of temperature that is not a real temperature and describes the sum of the interacting system's excitation degree and the influence of transverse flow at the kinetic freeze-

out stage. Briefly, the initial temperature is the highest and the kinetic freeze-out temperature is the lowest of the three temperatures, with the chemical freeze-out temperature falling somewhere in the middle which affects the pions' (bosons) energy density.

(ii) The thermodynamic of the nucleus-nucleus or proton-proton collisions is based on describing the manner of measurable macro-physical quantities such as the pseudo-rapidity and transverse momentum distribution of the produced particles with the statistical tool: “Tsallis’-Statics". It is to be stated here that Tsallis’ distribution function is a mathematical model used to describe the radiation and fragmentation in high-energy particle collisions. It is often used in the context of a heavy-ion collider. Based on that, the properties of the pseudo-rapidity distribution of produced particles have been figured out. It gives an overview of the experimental facilities that determine the spectra of the particles produced during a collision. Also, the Tsallis’ distribution can be used to determine the temperature at the kinetic freeze-out stage and to investigate the particle production process from the equilibrium degree in the system at different heavy ion collisions due to the centrality percentage. It is dragged from the classical Boltzmann-Gibbs statistics [11]. Such statistical methods provide us with information about the multiparticle production process and the equilibrium stages of the system till the freeze-out stage is reached. The bulk of matter created in high-energy collisions can be quantitatively described in terms of hydrodynamic and thermo-statistical models [13-14]. Tsallis’ distribution function is used to describe the distribution of measurable quantities such as pseudo-rapidity and transverse momentum distribution of produced charged

hadrons. Aiming to extract the average kinetic freeze-out temperature in a few sources which can describe local equilibrium states and the degree of non-equilibrium among different states.

Tsallis' distribution describes the thermal fluctuation of the system especially when this system has several sources that may exist in the hadron or heavy ion collision at high energies. Tsallis' form is used to describe the pseudo-rapidity distribution of produced charged hadrons [31]:

$$\frac{dN}{d\eta} = N_o \left[1 + (q-1)\frac{\sqrt{m^2+<p_t>^2\cosh^2(\eta)}}{T}\right]^{\frac{1}{1-q}} \frac{cosh(\eta)}{\sqrt{m^2<p_t>^{-2}+\cosh^2(\eta)}} \quad \text{... (10)}$$

Where T is the average kinetic freeze-out temperature in a few sources which can describe local equilibrium states, q is the non-equilibrium factor among different states, $<p_t>$is the average transverse momentum, m is the rest mass of produced charged particle (the mass of pion particle) and N_o is a normalization factor. The Values of q≈1 would indicate a system approaching equilibrium, while values greater than 1 indicate a system far from the equilibrium state.

It was necessary to modify equation (10) to fit the experimental data by adding two parameters; O and η_o to become more suitable in describing the experimental data as follows:

$$\frac{dN}{d\eta} = O + N_o \left[1 + (q-1)\frac{\sqrt{m^2+<p_t>^2\cosh^2(\eta-\eta_o)}}{T}\right]^{\frac{1}{1-q}} \frac{cosh(\eta-\eta_o)}{\sqrt{m^2<p_t>^{-2}+\cosh^2(\eta-\eta_o)}} \text{....} \quad (11)$$

Where O is the off-set parameter in the y-axis, η_o is a reference pseudo-rapidity. Equation (11) is used in describing the pseudo-rapidity distribution of produced charged hadrons in the interaction of ^{28}Si with the emulsion nuclei at 4.5 A GeV/c.

Tsallis' distribution could be formulated from several standard distributions as mentioned before. The used Tsallis' form is one of the simplest forms to describe

the probability density function of transverse momentum and rapidity[32],[33] Tsallis' double differential distribution $\frac{d^2N}{dydP_T}$is defined as:

$$\frac{d^2N}{dydP_t} = \frac{gV}{(2\pi)^2} P_t\sqrt{P_t^2 + m_0^2}\cosh(y)\left[1 + \frac{q-1}{T}\left(\sqrt{P_t^2 + m_0^2}\cosh(y) - \mu\right)\right]^{-\frac{q}{q-1}} \quad ...(12)$$

Where "g" is the degeneracy factor, "μ" is the chemical potential and m_o is the rest mass of the produced hadron due to quark recombination during the interaction. The following distribution form is chosen to describe the transverse momentum distribution at different rapidity intervals:

$$f(P_t, y) = C\, P_t\sqrt{P_t^2 + m_0^2}\, cosh(y)\ \left[1 + \frac{q-1}{T}\left(\sqrt{P_t^2 + m_0^2}\, cosh(y) - \mu\right)\right]^{-\frac{1}{q-1}} \quad ... (13)$$

While C=$\frac{gV}{(2\pi)^2}$ is the normalization constant and the factor $\frac{q}{q-1}$ can be replaced by $\frac{1}{q-1}$as the "q" value is usually close to 1. Then to fit the transverse momentum distributions of produced hadrons, equation (13) was used to deduce the values of chemical potential (μ), Temperature (T) and non-equilibrium index(q) at the kinetic freeze-out stage as fitting parameters. However, there is no chemical equilibrium at the kinetic freeze-out as the observed particle-antiparticle symmetry just indicates that the chemical potentials of particles must be equivalent to those of antiparticles[10].Therefore, the fit results of various proton-proton collisions are considered for non-zero chemical potential at the kinetic freeze-out stage. This procedure was applied to proton-proton collisions at GeV and TeV energy groups at all possible rapidity intervals. Accordingly, there are three fitting parameters for each rapidity interval describing its transverse momentum distribution. The results of the fitting will be discussed in the results section.

From another thermo-statistical perspective, giving more attention to the physics of non-equilibrium thermodynamic systems by solving the Vlasov time-dependent equation [34,35]:

$$\frac{df(t,r,P)}{dt} = \frac{\partial f}{\partial t} + \frac{\vec{P}}{m}.\vec{\nabla}_r f + \vec{\nabla}_r \mathrm{U}.\vec{\nabla}_p f \qquad (14)$$

Where $f(t,r,P)$ is the time-dependent wave function, while U(r) is a scalar potential acting among the particles. Assuming that the created quarks and gluons are produced in a spherical cloud with expandable volume according to the thermodynamic environment. Many approximations have been added so that equation (14) could be solved by considering a pre-equilibrium state where the time derivative df/dt may be approximated as $(f - f_0)/t_c$, where f_0 is the equilibrium distribution function, and t_c is the time interval required by the system to approach the equilibrium state. So, it is necessary to replace f with f_0 on the right-hand side of equation (14). Moreover, the particles are considered almost free so that the potential U could be neglected in this stage of approximation. The solution will be a power series, and for simplicity, it could be satisfied by using the first order only. So that equation (14) becomes:

$$f_1 = f_0 + t_c \frac{\vec{P}}{m} . \vec{\nabla}_r f_0 \qquad (15)$$

$$f_1(r) = f_0(r) + t_c \frac{p_t}{m \sin(\theta)} \cos\theta \frac{\partial f_0(r)}{\partial r} \qquad (16)$$

For the problem at hand, the transverse momentum distribution could be described as an exponential distribution, as follows:

$$f_0(P_t, r) = \gamma\, e^{-\frac{P_t}{T(r)}} \qquad (17)$$

as the radial dependence of $f_0(r)$ is included in the temperature gradient, $\partial T(r)/\partial r$. Assuming Gaussian density for the Quark-Gluon cloud of the form:

$$\rho(r) = A\,(\pi r)^{-\frac{3}{2}} e^{-\frac{r^2}{R^2}} \qquad (18)$$

with R is the virtual radius of the cloud and r being the distance measured from the center of the cloud. Now the temperature is very sensitive to the quark-gluon density ρ(r). So that the temperature gradient is written as:

$$\frac{\partial T(r)}{\partial r} = C \frac{\partial \rho(r)}{\partial r} \qquad (19)$$

where C is constant including the constants of equation (18) and the average kinetic energy of the particles in the cloud.

Then, equation (16) could be written as:

$$f_1(r) = f_0(r) + t_c \frac{P_t}{m} \cot(\theta) \frac{\partial f_0}{\partial T(r)} \frac{\partial T(r)}{\partial r} \quad (20)$$

Equation (20) is the power series solution of equation (14), which represents the equilibrium distribution with only a first-order approximation and the first term of the equation (20) is the zero-order approximation. The next term is the first correction term. The value of t_c is found by comparing equation (20) with the experimental $p_t$distribution at each rapidity interval.

Certain models among the theoretical models mentioned in the previous section in the analysis of nucleus-nucleus and nucleon-nucleon collisions at relativistic energies are a suitable approach to studying the presence of very hot and dense nuclear matter in the lab. For example, the properties of different secondary charged particles emitted in inelastic collisions of silicon nuclei with the nuclei of nuclear emulsion at the momentum of 4.5 A GeV/c have been investigated in the current work. In addition to that, it is a modest attempt to find some experimental signs of the phase transition from hadronic to Quark-Gluon Plasma state (QGP) by relating the change in the macroscopic variables such as transverse momentum, multiplicity distribution to the microscopic hypothesis of the transition mechanism.

Besides, the particle production had been studied from a macroscopic statistical respective that has made a large contribution to the success of experiments at the LHC energies and other heavy ion collisions in precision measurements of observables using "Tsallis' statistics" [11].

CHAPTER (III)
Experimental Data

III- Experimental Data:

A stack plate of Br-2 nuclear emulsions exposed to a 4.5 AGeV/c ^{28}Si beam at Dubna Synchro-Phastron of the intensity of irradiation » 10^4 particles/cm^2 and beam diameter » 1cm, was scanned by our group members under high power microscopes. Particle multiplicity, grain density and the emission angles of the emitted particles were accurately measured. According to the emulsion techniques [36], the tracks of the coming out secondary particles from the interactions were classified into black (slow), grey (intermediate) and shower (fast), according to their relative velocity β and specific ionization I*. The quantity $\beta=v/c$, where v and c are the particle velocity and speed of light. The quantity $I^*= I/I_o$, where I is the measured grain density of the secondary particle track (the number of developed grains in the photographic emulsion per 100 μm) and I_o is the grain density of the minimum ionizing particle track. These particles are emitted at space angles $q \leq 3^o$ and exposed to further multiple scattering measurements for momentum determination to separate the produced pions from the singly charged projectile fragments. These particles having, $I^*<1.4$ would have $\beta > 0.7$. This study was concerned about such single-charged fast particles being mostly produced as charged Pions. Which is compared with another experimental data of heavy ions as well as proton–proton collision experiments [37-40] that have a wide spectrum of collision energy.

CHAPTER (IV)
Results and discussion

IV- Results and discussion:

It might be convenient to start with some results of the simplest light ion collisions (p-p collisions) before going up to the heavy ion ones:

Figure (IV.1) presents the transverse momentum distribution (as a selected sample of all the available data of p-p reactions, since all of them show the almost same trend) of the produced hadrons in p-p collisions at 6.3 GeV for different rapidity regions. Different colored points belong to their corresponding rapidity value while lines are their fittings using the first order of solution of the Vlasov equation.

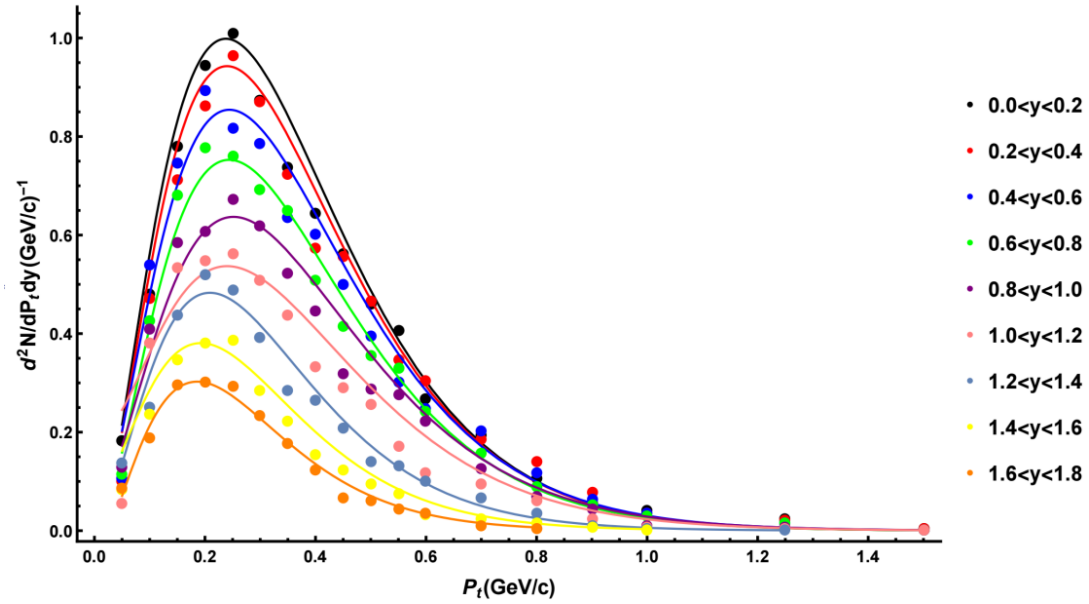

Fig. (IV.1): Transverse momentum distribution of the produced hadrons at 6.3 GeV at different rapidity slices. Lines are fittings using the first order of the Vlasov equation.

Fig. (IV.1) tells us that the Vlasov equation succeeds very well in describing the experimental data at all regions of rapidity. This fact was found to exist in all similar graphs in the ISR energy range, which would indicate some sort of local thermal equilibrium at these rapidity regions (at different deposition energy levels) that belong to one phase of nuclear matter.

This experimental fact tells us also that the produced particles follow a single mechanism of creation. It was considered to be a soft-creating mechanism that takes place between valence quarks in which every single final-state particle is produced and emitted independently. The produced particles in this mechanism, within this interaction energy, are thought to be almost pions, the multiplicity distribution of which follows a Poisson function, and their average values show a linear logarithmic relation with energy [41,42].

The time taken by the system to approach the equilibrium state, t_c was found by comparing equation (20) with the experimental values of the transverse momentum,$p_t$distribution at each rapidity interval. The values that show up in Table (I), say that the temperature rises up as the rapidity goes towards the center, so that particles emitted in the forward direction are created in early time with low temperature and far from equilibrium (longer t_c). In other words, the quarks and gluons interact together in a small volume of a cloud. The quarks passing in parallel trajectories and having nearby momentum can recombine together forming hadrons emitted in the forward direction with a relatively low temperature in a non-equilibrium state. The cloud expands gradually with increasing the frequency of collisions and the emission is produced at a wider solid angle, i.e. (smaller values in rapidity space) with increasing temperature, the system approaches an equilibrium state.

Table (I): Values of the parameters T and t_c for pions produced in p-p collisions at 6.3 GeV.

Rapidity interval	T(GeV)	t_c (fm/c)
$0.0 < y < 0.2$	0.129	3.46
$0.2 < y < 0.4$	0.120	15.0
$0.4 < y < 0.6$	0.115	20.3
$0.6 < y < 0.8$	0.112	28.8
$0.8 < y < 1.0$	0.110	32.5
$1.0 < y < 1.2$	0.104	39.5
$1.2 < y < 1.4$	0.100	48.0
$1.4 < y < 1.6$	0.096	54.8
$1.6 < y < 1.8$	0.091	65.9

More expansion of the cloud and more frequency of particle collisions may cause the stability of the temperature that reaches equilibrium.

The above point of view is supported by the relation between the entropy (indicated by the rapidity density) of the produced particles and the temperature of the interaction zone (indicated by the average transverse momentum) [17,19] and presented in the central rapidity region by figure (IV.2):

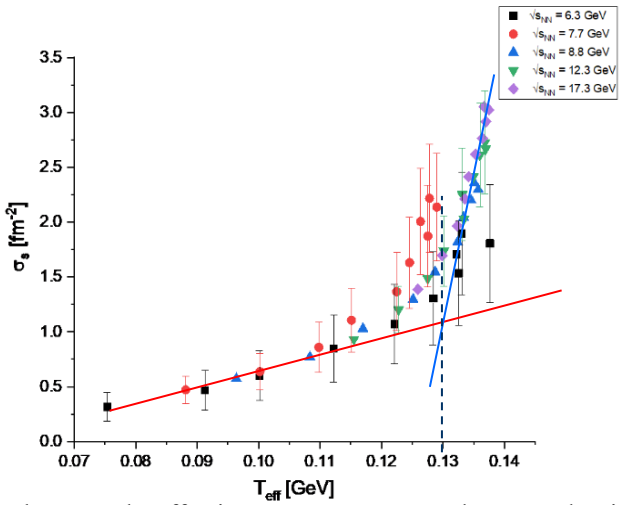

Fig. (IV.2): the relation between the effective temperature T_{eff} and entropy density σ_s for some ISR interaction energy at central rapidity range (y = 0.0 - 2.0).

In figure (IV.2), one would notice a good agreement between the data in the stated interaction energy region, supporting that the created particles and the medium lie under the same thermodynamic condition or in other words, the production mechanism takes place in one phase of nuclear matter.

Looking for changes in the state of nuclear matter at higher category of interaction energy; the relation between the entropy and temperature is presented in figure (IV.3).

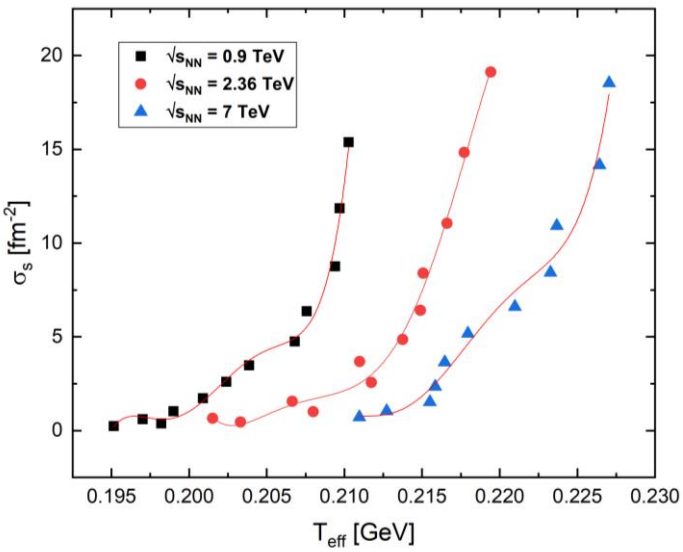

Fig.(IV.3): the correlation between the effective temperature T_{eff} and entropy density σ_s of charged hadrons produced in p-p collision at $\sqrt{s}$ = 0.9, 2.36 and 7 TeV.

The relations in figure (IV.3) exhibit more than one remarkable feature; 1st, each interaction energy data of the presented values follows a separate independent relation, and 2nd, it is noticed also a couple of irregularities in these relations. So, one might be led to think of more than one relation, between entropy and the temperature, for different interaction energies.

This could be attributed to different states of nuclear matter or different thermodynamic conditions in which the produced particles are created.

There is also a possibility that other species of particles have taken part in the creation, as a higher energy deposit would give the possibility of creating heavier quarks allowing keons, lambdas and other particles to show up.

In fact, there might not be sharp borders between the phases or modes where nuclear matter is transferred from one to another, but the experimental results together with theoretical models have been always helping to figure out what happens in the nuclear matter as the thermodynamic conditions change by raising the interaction energy or by increasing centrality of collisions. It can be understood that as energy goes higher, nucleons could be viewed as bundles of valence quarks and gluons. At enough energy, interaction between these quarks leads to a production of other quarks called sea quarks and as energy gets even higher, interactions between quarks and gluons start to take place and interaction between gluons themselves is added to all of the above ones. These modes of interactions are probably thought to be responsible for the large rise in multiplicity of the created particles allowing heavier particles than pions to be produced, thus, changing the relations between experimental physical quantities and the outlines that describe them.

As was stated in the introduction; the fitting of Tsallis' distribution function with the experimental data of the double differential distribution $d^2N/dydp_t$was used to obtain the values of the three parameters; namely, temperature, chemical potential and the non-equilibrium factors (entropy index) at each rapidity interval of the pp collisions, each at its corresponding center of mass energy of the values of energy under investigation. Fig. (IV.4) shows the dependence of the chemical potential μ on the temperature T.

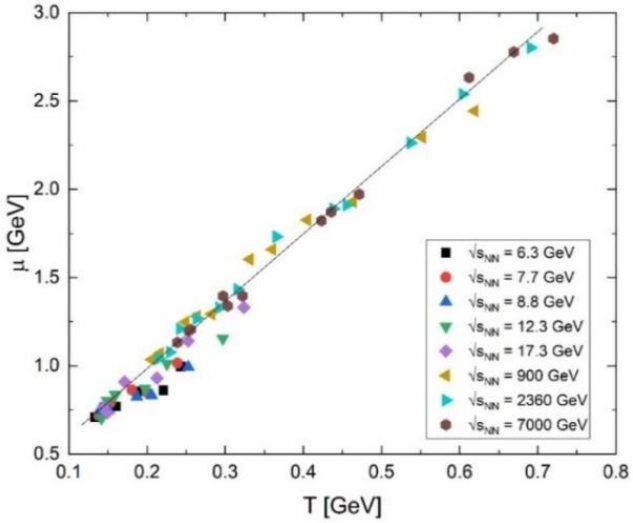

Fig. (IV.4): μ-T phase diagram of particles produced in the final state of p-p collisions at different centres of mass energies. The line is fit for the data.

In figure (IV.4), one would notice that the dependence of the chemical potential values on the temperature follows nicely a linear relation given as:

$$\mu = b\,T + \mu_0 \ldots \quad (21)$$

With fitting parameters, b = 3.8 and μ_0 = 0.62.

Where μ_0 is a reference chemical potential and b, the slope of the line, reveals a constant chemical potential change per unit change of the temperature of the nuclear medium. This fact may point to a continuous transition, in analogue to a second order of the QCD phase, which would also tell us that as the centrality of interaction increases, more energy would be deposited into the system, leading to a rise of its temperature and creation of more particles. This could also be physically accepted on the bases that in the phase through which the nuclear matter is passing in the considered range of energy, more kinetic energy is gained by the created particles, thus, increasing the free energy of the system for higher

interaction energy. This occurs when the chemical potential exceeds much more the pion mass and corresponds to the pion condensation [43].

However, one may observe in figure (IV.4), that some data points do not stick will to the fitting line in the temperature range ~ 0.2 to 0.3 GeV. This may be attributed to the inclusion of mixed phases that exist in this temperature range or more than one species of particles are produced in this region or an unbalanced state between the absorbed and emitted energy of the particles content (e.g., a latent heat energy of releasing more sea quarks or even condensate of sea quarks to form particles).

The relation between the temperature of the system and the rapidity of the produced particles is presented in figure (IV.5):

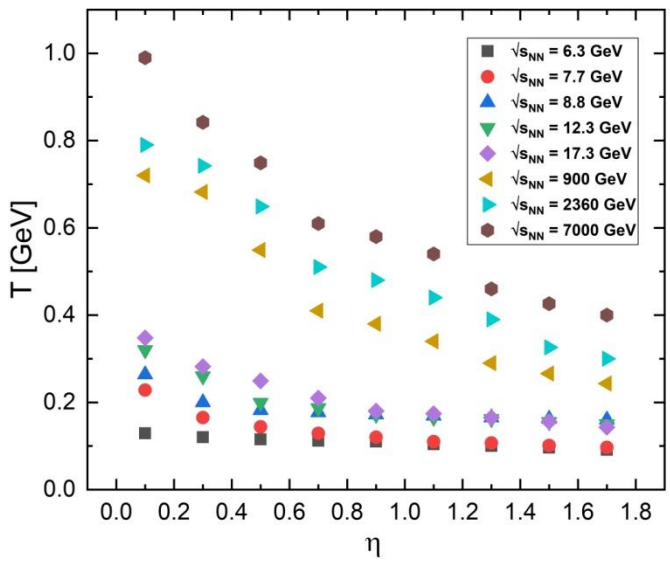

Fig. (IV.5): Variation of the temperature with pseudo-rapidity of produced particles in p-p collision.

In figure (IV.5), one can see that the temperature decreases gradually with the rapidity from the central collision region (low rapidity) down to high rapidity for

all the data considered in this study. The temperature falls more rapidly with the rapidity in the TeV group than for the GeV ones.

The temperature versus pseudo-rapidity curves shift up for the TeV group where more energy is available. One may come up with the fact that particles produced in the most forward direction (high rapidity intervals) are produced at low temperature and far from equilibrium. As particles spread out toward the central region with small rapidity, the final state is attained with a larger temperature and approaches the pre-equilibrium. This means that as time goes on, particles are produced in a larger cone angle (smaller rapidity) and due to the successive quarks-gluons interactions both the temperature and entropy increase, hence the system approaches equilibrium.

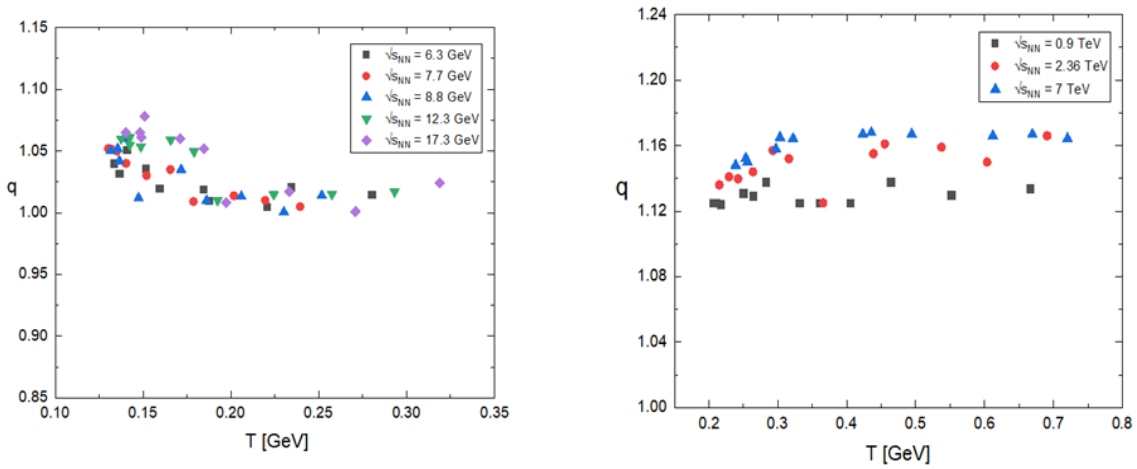

(a) (b)

Fig. (IV.6): the dependence of the non-equilibrium parameter q on the temperature T for particles produced in p-p collision for the: GeV energy group in fig. (IV.6-a) and TeV energy group in fig. (IV.6-b).

The features of the graphs in Figure (IV.6) may be consistent with what came out from figure (IV.5). In figure (IV.6-a); at the beginning of particle emission, the system has relatively large q values for temperature below 0.2 GeV, which are far

from equilibrium. As time goes on, the temperature rises, and the system approaches equilibrium (q » 1). In the temperature range between 0.2 and 0.3 GeV, q shows lower values tending to be somehow closer to equilibrium. This trend looks the same for the data for center of mass energies at few GeVs. In figure (IV6-b); one would notice some kind of steady q-T relations for the TeV group for T above 0.3 GeV of data at different levels (shown by the colored guidelines). All these levels are far from equilibrium with larger values for higher interaction energies.

In the next part, one would see how some of the studied physical parameters investigated above in p-p collisions, would look like in heavy ion ones. The rapidity distribution of the produced particles in a nuclear reaction refers to the size of the reaction and the origin of the produced particles. Figure (IV.7) shows schematic features of such parameters at different classes of heavy ion interaction energy [44].

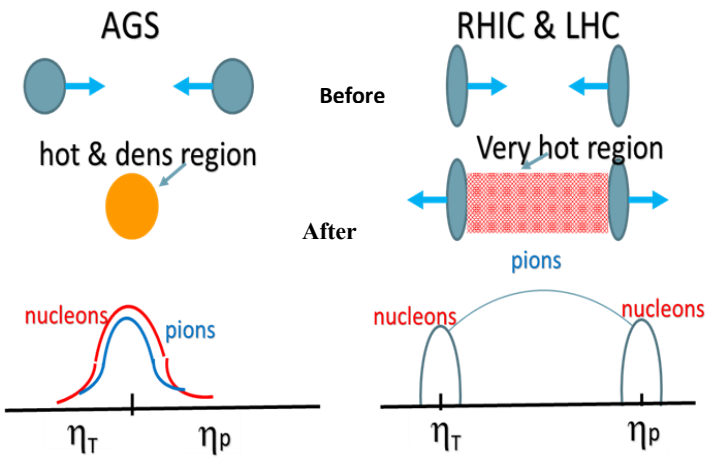

(a) (b)

Fig. (IV.7): a schematic diagram of the origin of pseudo-rapidity of the produced particles in heavy ion collisions in the AGS energy region fig. (IV.7-a) and in the RHIC and LHC one fig. (IV.7-b).

In fig.(IV.7-a), around Alternating Gradient Synchrotron(AGS) energy region, the colliding nuclei stop each other forming a hot baryon rich volume in the middle, while in fig.(IV.7-b), in the Relativistic Heavy Ion Collider (RHIC) and the Large Hadron Collider (LHC) energy regions, the Lorenz-contracted nuclei penetrate through each other forming a very hot baryon-free volume in the middle. In fig.(IV.7), h_p and h_T indicates the projectile and target rapidity, respectively.

The pseudo-rapidity of the produced charged hadrons is calculated using the measured space angle q_s of the fast charged hadrons according to the formula:

$$\eta = -\ln(\tan(\frac{\theta_s}{2}))\ldots (22)$$

Figure (IV.8) presents η- distributions of produced charged particle through the interaction of ^{28}Si with emulsion nuclei at 4.5 A GeV/c, for four degrees of centrality, classified according to the total charge of the non-interacting charged particles Q, as follows:

central: Q = (0-1)

semi-central: Q = (2-5)

semi- peripheral: Q = (6-10)

peripheral: Q = (11-14)

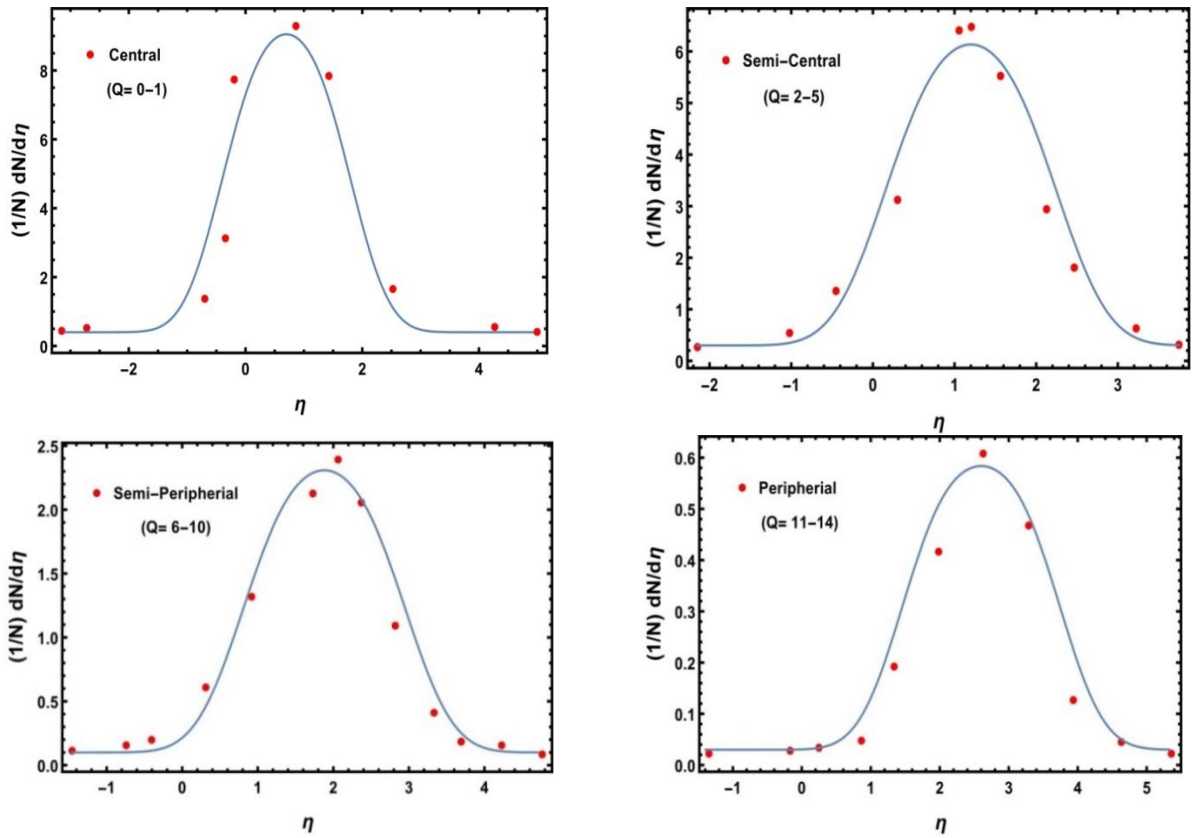

Fig.(IV.8): Pseudo-rapidity distribution of the shower particles emitted in 4.5A GeV/c ^{28}Si-Em Interactions for central, semi-central, semi-peripheral and peripheral collisions.

Figure (IV.8) shows that each one of the rapidity distributions appears as one Gaussian function, as expected at that relatively low interaction energy. This Gaussian distribution contains three mixed Gaussians inside it; one from the fireball and the other two from the fragmentation of the projectile and target sources, according to the three-source model [45]. At the center of mass interaction energy values $s_{NN} \leq 20$ GeV, these three distributions reduce to the two fragmentation sources due to the very low effect of the gluonic source.

The three stated distributions from their emitting sources get dispersed from each other as that of the AGS energy region. This dispersion spreads more and more, further apart, as the collision energy passes through the RHIC and enters the LHC values [48]. Some parameters from the equivalent Gaussian fit to the data of figure (IV.8) have been extracted and presented in table (II) to help in the quantitative description of the data:

Table (II): Parameters from the equivalent Gaussian fit to the pseudo-rapidity distribution of the shower particles emitted in 4.5A GeV/c ^{28}Si-Em Interactions for central, semi-central, semi-peripheral and peripheral.

Interaction type	peak hight	peak position	Peak width
Peripheral	0.65	2.6	1.27
Semi-peripheral	2.5	1.8	1.42
Semi-central	6.2	1.2	1.46
Central	9.0	0.86	1.58

From figure (IV.8) and table (II), one may notice that, as we move from peripheral to central collisions:

a- The peak value of the rapidity gets higher. This could be referred to the increase in the number of participants from both the interacting nuclei. This causes a larger amount of deposited energy in the interaction region and hence a greater number of created particle multiplicity, according to the principle of the "participant scaling" [46].

b- The peak position shifts towards the lower values. This might be attributed to the increase in the number of collisions that increases the values of the transverse momentum of the interacting and created particles leading to wider scattering angles of the coming out particles.

c- The width of the distributions gets fatter by a small amount, as would be expected from the widening of the gap between the projectile and target participants particle sources, in the rapidity space. Assuming that at high

energy, the two interacting nuclei can be viewed as two groups of individual nucleons. Then, according to the "Thermalized Cylinder Model" [21] which uses the simple picture of the one-dimensional "string" model [47] and the "fireball" model [15]; the "string" model assumes that in relativistic nucleon-nucleon collisions, a string is formed consisting of two endpoints acting as energy reservoirs and the interior with constant energy per length. The string breaks into several substrings along the direction of the incident beam. The distribution length of substrings will define the width of the pseudo-rapidity distribution. The "fireball" model assumes that the incident nucleon penetrates through the target nucleon, and then a fire-streak is formed along the direction of the incident beam. The length of the fire-streak expresses the width of the pseudo-rapidity distribution. As the energy content in the collision gets larger; greater number of strings or Fire-streaks are formed along the incident direction. The "Thermalized Cylinder Model" assumes that these strings or Fire-streaks mix in the transverse direction; thus, leading to increases in the width of the distribution as one moves from the peripheral to central collisions. However, the ^{28}Si–Emulsion data show small increases in the width as is expected in this relatively low interaction energy, in which expansion of the interaction volume does not increase drastically, relative to that expected to happen at the RHIC and the LHC energies.

Table (III) below, shows the values of kinetic freeze-out temperature T, the average transverse momentum $< p_{\mathrm{t}} >$, the non-equilibrium factor q and the entropy density extracted as fitting parameters from Tsallis' distribution function equation (13) for each interaction type. The entropy density was calculated from equation (6).

Table (III): Values of kinetic freeze-out temperature T, average transverse momentum $< p_t >$, the non-equilibrium factor q and the entropy density.

Interaction type	T (MeV)	$< p_t >$ (MeV/c)	q	N_o	η_o	o	$<\sigma_s>$ (fm^{-2})
Peripheral	101	156	1.034	5.5	2.6	0.03	0.07
Semi-peripheral	105	172	1.030	22	1.9	0.10	0.18
Semi-central	115	187	1.028	52	1.2	0.30	0.37
Central	134	192	1.025	60	0.7	0.40	0.43

There are some facts that manifest themselves in table(III), as the centrality of collision increases. These facts may be summarized as follows:

(i) The temperature of the emitting particle system rises due to increasing average values of transverse momentum with a consequence of a larger amount of deposited energy in the interaction region, thus, higher temperature.

(ii) The entropy density increases to probably indicate a slow gradual hadron dissociation, forming quark pairs, and getting into the QGP phase. So, we have a situation of a growing number of created particles and an increased amount of content in the interaction volume.

(iii) The non-equilibrium factor, q, looks to be decreasing with very small values as the centrality increases tending to approach equilibrium. This behavior may be understood in view of the fact that, in the peripheral collision, particles are produced in the most forward direction (high rapidity intervals, having small transverse momenta and low entropy density) at low temperature and a little bit far from equilibrium. As centrality increases, particles spread out with small rapidity to attain the final state with larger temperature and closer to

pre-equilibrium. In other words, deeper centrality of interaction means a longer time for the particles to stay in the system, with increased quark-gluon interactions, be produced in larger cone angle (smaller rapidity), leading to higher temperature and larger entropy, and become closer to equilibrium. However, all the q values of the ^{28}Si–Emulsion data at 4.5 GeV/c, are pretty close to unity, indicating a good equilibrium state for the whole interacting system at this interaction energy.

On the other hand, the extracted values of non-equilibrium index q of the ^{28}Si–Emulsion data, compared with that of other heavy ion collisions [37-40] using Tsallis distribution function, as shown in figure (IV.9).

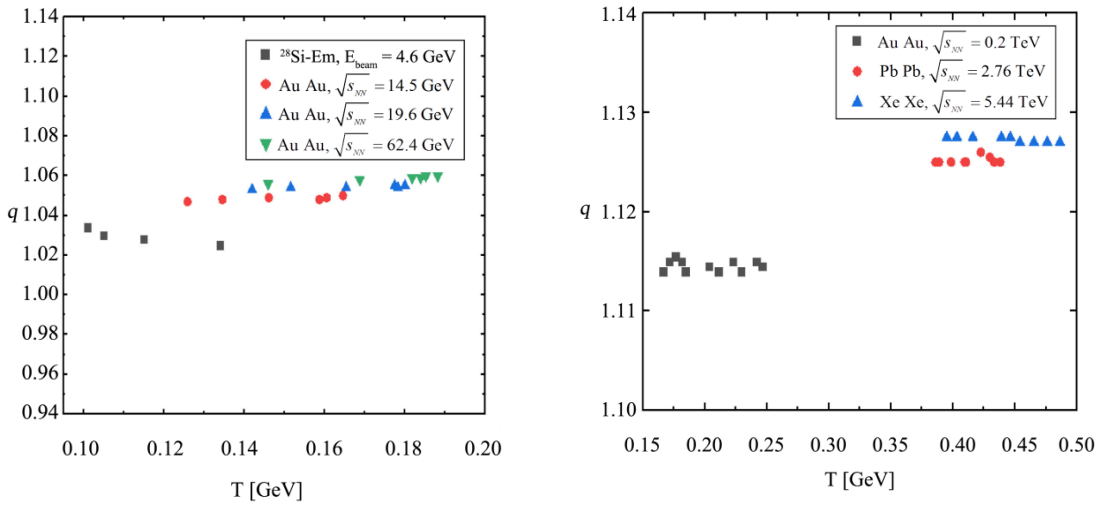

Fig. (IV.9) The change of the non-equilibrium parameter q with the temperature T of the produced particles in heavy ion collisions for GeV fig. (IV.9-a) and TeV group of energy fig.(IV.9-b).

It is noticeable from fig.(IV.9-a) that q increases by a very small rate with the temperature in the stated range of interaction energy, keeping fairly close to the equilibrium state of the interacting system.

While in fig.(IV.9-b) the non-equilibrium parameter q has different levels of saturations that get higher as the interaction energy increases, meaning that such saturation levels get further apart from the equilibrium level for higher interaction energy. This might be interpreted by recalling the fact that at such high energy density of the system, there is no way the matter could be tightly packed as a collection of hadrons but, instead, it is a gas of quarks and gluons. The interaction between these quarks and gluons is very weak and the equilibrium state of matter is far to be reached, as could be imposed by the interplay between the two crucial characters of the QCD: the color confine and the asymptotic freedom [47].

Previous results are focused on studying the low transverse momentum spectra of certain species of charged particles based on Tsallis statistics. However, the study could be extended by applying the Tsallis approach to a wider dataset that includes more heavy hadrons across various centralities and beam energies. It would provide insights into how the degree of non-equilibrium and effective thermal conditions vary with particle mass and strangeness content. Technically, the fitting procedure could be improved by including collective flow effects. The radial (transverse) flow significantly influences the shape of the low-pT spectra, particularly for heavier hadrons . Accordingly, it contributes to formulating an accurate particle production interpretation. For instance, the implementation of the Tsallis Blast-Wave model, which embeds a radial flow velocity influence to enable the simultaneous extraction of thermal and collective parameters, including the average transverse flow velocity [14,48]. Therefore, it improves the fitting quality and enhances the phenomenological relevance of the extracted quantities. Such further extensions of the study would not only improve the robustness of the current analysis but also provide a broader vision of the particle production, collective behavior, and QCD thermodynamics throughout different collision systems.

CHAPTER (V)

CONCLUSION

V. CONCLUSION

According to the thermodynamic features revealed by the experimental data investigated in this thesis, in view of related theoretical models, one could arrive at a group of facts that can be summarized as follows:

- The produced charged particles through a few tens of GeV energy of p-p collision probably follow from a crossover transition through a certain production mechanism , wherein the fireball remains instantaneous, and the system evolves smoothly, maximising entropy and particle multiplicity. This smooth transition indicates a rapid freezing out of the QGP phase into the hadron phase. Furthermore, such a feature emphasises the idea of the system smoothly transitioning through equilibrium, enhancing the production of the lightest mesons (pions).Whereas, at a higher range of energy, it could be more than one particle production mechanism, relying on the nature of transitions that the nuclear matter goes through in the phase diagram between certain thermodynamic parameters, such as in figure(IV.3). It could be explained by the interactions between valence quarks, which lead to producing another type of hadron that is different from those produced in the tens of GeV range. As energy goes higher, interactions between valence quarks and sea quarks seemed to take place. At even higher levels of energy, more species of particles are created as a consequence of quark-gluon and gluon-gluon interactions that are added to the other mentioned ones.
- The analysis of the experimental data in view of Tsallis' statistics has enabled one to obtain the values of the temperature, chemical potential, and non-equilibrium factor of the nuclear system as fitting parameters at each center of mass energy of the GeV and TeV data groups. For the pp

data; at the GeV energy region; the chemical potential changes linearly with the temperature of the particle emitting system. The regular relationship between these two parameters for temperature above 0.20 GeV indicates certain species of the produced particle is dominating and created according to one mechanism. For T less than 0.20 GeV the relation is not perfectly linear, thus, indicating the existence of more than one phase of nuclear medium and more than one mechanism is taking part in particle creation stage.

- The temperature-rapidity graphs show that the temperature decreases gradually with rapidity, with maximum temperature at zero rapidity (central part). This is common for collisions at all energy ranges. The temperature falls more rapidly with rapidity in the TeV region than in the GeV region.
- The non-equilibrium parameter shows small bits of decreases with centrality approaching equilibrium in the ^{28}Si–Emulsion data . In a few tens of GeV of interaction energy, the systems keep, somehow, close to the border of equilibrium with small bits of getting further from it. In the TeV energy, this parameter has shown different levels of saturations that get away from the equilibrium value and from each other as the interaction energy gets higher and higher.

REFERENCES

REFERANCES:

[1] HotQCD Collaboration (2019) Chiral Crossover in QCD at Zero and Non-Zero.Chemical Potentials. Physics Letters B , 795, 15-21. https://doi.org/10.1016/j.physletb.2019.05.013

[2] Ahmad, M.A. (2017) Some Aspects of Simulations and Modeling in Relativistic Nuclear Collisions (Astro-Particle Physics). International Journal of High Energy Physics , 4, 58-64. https://doi.org/10.11648/j.ijhep.20170405.12

[3] McLerran, L. and Pisarski, R.D. (2007) Phases of Dense Quarks at Large Nc . Nuclear Physics A , 796, 83-100. https://doi.org/10.1016/j.nuclphysa.2007.08.013

[4] McLerran, L. and Reddy, S. (2019) Quarkyonic Matter and Neutron Stars. Physical Review Letters , 122, Article ID: 122701. https://doi.org/10.1103/PhysRevLett.122.122701

[5] Daftari, I.K. and Roy, T. (1978) Some Observations on Coplanar Decay of Fireballs at 24 GeV/c Proton-Nucleus Interaction. Czechoslovak Journal of Physics B, 28,521-528. https://doi.org/10.1007/BF01597201

[6] Hussen, M.T., Rabea, A., El-Naghy, A. and Hassan, N.M. (1995) A String Model for Hadron Interactions at High Energies. Progress of Theoretical Physics , 93, 585-595.https://doi.org/10.1143/ptp/93.3.585

[7] Tao, J., Wu, W., Wang, M., Zheng, H., Zhang, W., Zhu, L. and Bonasera, A. (2022) The Novel Scaling of Tsallis Parameters from the Transverse Momentum Spectra of Charged Particles in Heavy-Ion Collisions. Particles, 5, 146-156. https://doi.org/10.3390/particles5020013

[8] Hussein, M.T., Ghoneim, M.T. and Abdel-Halim, Z. (2022) Signs of Phase Transition in High Energy Proton-Proton Collisions. Journal of Applied Mathematics and Physics, 10, 1887-1897. https://doi.org/10.4236/jamp.2022.106129

[9] Tirnakli, U. and Borges, E.P. (2016) The Standard Map: From Boltzmann-Gibbs Statistics to Tsallis Statistics. Scientific Reports, 6, Article No. 23644. https://doi.org/10.1038/srep23644

[10] Cleymans, J. and Paradza, M.W. (2020) Determination of the Chemical Potential in theTsallis Distribution at LHC Energies. High Energy Physics: Phenomenology. http://arxiv.org/abs/2010.05565

[11] Tsallis, C. (2019) Beyond Boltzmann-Gibbs-Shannon in Physics and elsewhere. Entropy, 21. https://doi.org/10.3390/e21070696

[12] Li, B.C., Bai, T., Guo, Y.Y. and Liu, F.H. (2017) On J/ψ and γ Transverse Momentum Distributions in High Energy Collisions. Advances in High Energy Physics,2017, Article ID: 9383540. https://doi.org/10.1155/2017/9383540

[13] Shao, M., Yi, L., Tang, Z., Chen, H., Li, C. and Xu, Z. (2010) Examination of the Species and Beam Energy Dependence of Particle Spectra Using Tsallis Statistics.Journal of Physics G: Nuclear and Particle Physics, 37, Article 058104. https://doi.org/10.1088/0954-3899/37/8/085104

[14] Tang, Z., Xu, Y., Ruan, L., van Buren, G., Wang, F. and Xu, Z. (2009) Spectra and Radial Flow in Relativistic Heavy Ion Collisions with Tsallis Statistics in a Blast-Wave Description. Physical Review C: Nuclear Physics, 79, Article 051901. https://doi.org/10.1103/PhysRevC.79.051901

[15] Westfall, G. D., Gosset, J., Johansen, P. J., Poskanzer, A. M., Meyer, W. G., Gutbrod, H. H., Sandoval, A., & Stock, R. (1976) Nuclear Fireball Model for proton inclusive spectra from relativistic heavy-ion collisions. Physical Review Letters, 37(18), 1202–1205. https://doi.org/10.1103/PhysRevLett.37.1202

[16] Mobed, N., & Gupta, S. Das. (1983) Firestreak model. Phys. Rev. C, 27(4), 1526–1531.https://doi.org/10.1103/PhysRevC.27.1526

[17] Fermi, E. (1950) High Energy Nuclear Events. Progress of Theoretical Physics, 5,570-583. https://doi.org/10.1143/ptp/5.4.570

[18]Landau, L. D. (1953) On the multiparticle production in high-energy collisions. *Izv. Akad. Nauk Ser. Fiz*, *17*(51), L021902-6.

[19] Martinez, G. (2013) Advances in Quark Gluon Plasma. e-Print: 1304.1452 [nucl-ex]. https://doi.org/10.48550/arXiv.1304.1452.

[20] Campanini, R., &Ferri, G. (2018) Experimental equation of state in pp and $\bar{p}$ p collisions and phase transition to quark gluon plasma.Physics Letters B,703, 3, 237-245. https://doi.org/10.1016/j.physletb.2011.08.009

[21] Liu, F.H. (1999) Pseudorapidity (Rapidity) Distribution of Shower Particles in Relativistic Nucleus-Nucleus Collisions. Il Nuovo Cimento A, 112, 1167-1179. https://doi.org/https://doi.org/10.1007/BF03035920

[22] Liu, F. H., &Panebratsev, Y. A. (1998) Pseudorapidity distribution shape of shower particles in high energy nucleus-emulsion collisions. Nuclear Physics A, 641(3), 379–385. https://doi.org/10.1016/S0375-9474(98)00475-8

[23] Mekjian, A. (1978) Statistical thermodynamics of relativistic heavy ion collisions. 312, 491–523.https://doi.org/10.1016/0375-9474(78)90604-8

[24] Das Gupta, S., &Mekjian, A. Z. (1981) The thermodynamic model for relativistic heavy ion collisions. Physics Reports, 72(3), 131–183. https://doi.org/10.1016/0370-1573(81)90012-0

[25] Koch, V. (2003) Some remarks on the statistical model of heavy ion collisions. Nuclear Physics A, 715, 108c–117c. https://doi.org/10.1016/S0375-9474(02)01419-7

[26] Adams, J., Aggarwal, M. M., Ahammed, Z., Amonett, J., Anderson, B. D., Arkhipkin, D., Averichev, G. S., Badyal, S. K., Bai, Y., Balewski, J., Barannikova, O., Barnby, L. S., Baudot, J., Bekele, S., Belaga, V. V., Bellingeri-Laurikainen, A., Bellwied, R., Berger, J., Bezverkhny, B. I., … Zubarev, A. N. (2005) Experimental and theoretical challenges in the search for the quark-gluon plasma: The STAR Collaboration's critical assessment of the evidence from RHIC collisions. Nuclear Physics A, 757(1-2 SPEC. ISS.), 102–183. https://doi.org/10.1016/j.nuclphysa.2005.03.085

[27] Baker, O. K. and Kharzeev, D. E.. (2018) Thermal radiation and entanglement in proton-proton collisions at energies available at the CERN Large Hadron Collider.Phys. Rev. D,98,05400.https://link.aps.org/doi/10.1103/PhysRevD.98.054007

[28] Gardim, F. G., Giacalone, G., Luzum, M., &Ollitrault, J. Y. (2020) Thermodynamics of hot strong-interaction matter from ultrarelativistic nuclear collisions. Nature Physics, 16(6), 615–619. https://doi.org/10.1038/s41567-020-0846-4

[29] Basu, S., Nandi, B.K., Chatterjee, S., Chatterjee, R. and Nayak, T. (2016) Beam Energy Scan of Specific Heat through Temperature Fluctuations in Heavy Ion Collisions. Journal of Physics: Conference Series, 668, Article ID: 012043. https://doi.org/10.1088/1742-6596/668/1/012043

[30] Filinov, V. and Larkin, A. (2019) Momentum Distribution Functions in QuarkGluon Plasma. Journal of Applied Mathematics and Physics, 7, 1997-2014. https://doi.org/10.4236/jamp.2019.79137

[31] Rybczyński, M. and Włodarczyk, Z. (2020) Inelasticity Resulting from Rapidity Spectra Analysis. New Journal of Physics, 22, Article 113002. https://doi.org/10.1088/1367-2630/abc1ca

[32] Lao, H., Wei, H., Liu, F. and Lacey, R.A. (2016) An Evidence of Mass Dependent Differential Kinetic Freeze-Out Scenario Observed in Pb-Pb Collisions at 2.76 TeV. The European Physical Journal A, 52, Article No. 203. https://doi.org/10.1140/epja/i2016-16203-2

[33] Si, R.F., Li, H.L. and Liu, F.H. (2018) Comparing Standard Distribution and Its Tsallis Form of Transverse Momenta in High Energy Collisions. Advances in High Energy Physics , 2018, Article ID: 7895967. https://doi.org/10.1155/2018/7895967

[34] Hussein, M.T., Hassan, N.M. and El-Harby, N. (2000) Time Evolution of Fast Particles during Decay of Hadronic Systems. Turkish Journal of Physics , 24, 501-511.

[35] Haque, M. I., Tariq, M., Jahan, H., & Hussain, T. (2014) Some Aspects of Multiparticle Production in Relativistic Nuclear Collisions. Journal of Modern Physics, 05(14), 1353–1359. https://doi.org/10.4236/jmp.2014.514136

[36] Eberhard, P.H. (1961) Parameters of the $K_o\overline{K_o}$ System. Physical Review Letters,16, 150-153. https://doi.org/10.1103/PhysRevLett.16.150

[37] STAR Collaboration, Adamczyk, L., Adams, J.R., Adkins, J.K., Agakishiev, G., Agarwal, M.M., Ahammed, Z., Ajitanand, N.N., Alekseev, I., Anderson, D.M., Aoyama, R., Aparin, A., Arkhipkin, D., Aschenauer, E.C., Ashraf, M.U., Attri, A., Averichev, G.S., Bai, X., Bairathi, V. and Zyzak, M. (2017)

Beam Energy Dependence of Jet-Quenching Effects in Au+Au Collisions at $\sqrt{s_{NN}}$ = 7.7, 11.5, 14.5, 19.6, 27, 39 and 62.4 GeV. Physical Review Letters, 121, Article 032301. https://doi.org/10.1103/PhysRevLett.121.032301

[38] Adler, S.S., Afanasiev, S., Aidala, C., Ajitanand, N.N., Akiba, Y., Alexander, J., Amirikas, R., Aphecetche, L., Aronson, S. H., Averbeck, R., Awes, T.C., Azmoun, R., Babintsev, V., Baldisseri, A., Barish, K.N., Barnes, P.D., Bassalleck, B., Bathe, S., Batsouli, S. and Zolin, L. (2004) Identified Charged Particle Spectra and Yields in Au +Au Collisions at $\sqrt{s_{NN}}$ = 200 GeV. Physical Review C, 69, Article 034909. https://doi.org/10.1103/PhysRevC.69.034909

[39] Acharya, S., Acosta, F. T., Adamová, D., Adolfsson, J., Aggarwal, M. M., Aglieri Rinella, G., Agnello, M., Agrawal, N., Ahammed, Z., Ahn, S. U., Aiola, S., Akindinov, A., Al-Turany, M., Alam, S. N., Albuquerque, D. S. D., Aleksandrov, D., Alessandro, B., Alfaro Molina, R., Ali, Y., … Zou, S. (2018) Transverse momentum spectra and nuclear modification factors of charged particles in pp, p-Pb and Pb-Pb collisions at the LHC. Journal of High Energy Physics, 2018(11). https://doi.org/10.1007/JHEP11(2018)013

[40] Acharya, S., Acosta, F.T., Adamová, D., Adolfsson, J., Aggarwal, M.M., Aglieri Rinella, G., Agnello, M., Agrawal, N., Ahammed, Z., Ahn, S.U., Aiola, S., Akindinov, A., Al-Turany, M., Alam, S.N., Albuquerque, D.S.D., Aleksandrov, D., Alessandro,B., Alfaro Molina, R., Ali, Y. and Zou, S. (2019) Transverse Momentum Spectra and Nuclear Modification Factors of Charged Particles in Xe-Xe Collisions at $\sqrt{s_{NN}}$ = 5.44 TeV. Physics Letters B, 788, 166-179. https://doi.org/10.1016/j.physletb.2018.10.052

[41] Z. Koba, H.B. Nielsen, P. Olsen (1972) Scaling of multiplicity distributions in high energy hdron collisions .Nucl. Phys. B40 ,317-334.https://doi.org/10.1016/0550-3213(72)90551-2

[42] Bravina, L. V., &Zabrodin, E. E. (2016) Scaling trends in proton-proton collisions from SPS to LHC in quark-gluon string model. Journal of Physics: Conference Series, 668(1). https://doi.org/10.1088/1742-6596/668/1/012045

[43] Nishihara, H. and Harada, M. (2013) Enhancement of Chiral Symmetry Breaking from the Pion Condensation at Finite Isospin Chemical Potential in a Holographic QCD Model. Physical Review D, 89, Article 076001. https://doi.org/10.1103/PhysRevD.89.076001

[44] Nagamiya, S. (2022) Heavy-Ion Collisions toward High-Density Nuclear Matter. Entropy, 24, 482. https://doi.org/10.3390/e24040482

[45] Csernai, L.P., Lovas, I., Maruhn, J.A., Rosenhauer, A., Zimanyi, J. and Greiner, W.(1982) Three-Component Fluid Dynamics for the Description of Energetic Heavy-Ion Reactions. Physical Review C, 26, 149-161. https://doi.org/10.1103/PhysRevC.26.149

[46] Busza, W., Rajagopal, K. and van der Schee, W. (2018) Heavy ion Collisions: The Big Picture and the Big Questions. Annual Review of Nuclear and Particle Science,68, 339-376. https://doi.org/10.1146/annurev-nucl-101917-020852

[47] Werner, K. (1993) Strings, Pomerons and the venus Model of Hadronic Interactions at Ultrarelativistic Energies. Physics Reports, 232, 87-299. https://doi.org/10.1016/0370-1573(93)90078-R

[48] Chen, J., Deng, J., Tang, Z., Xu, Z. and Yi, L. (2021). Nonequilibrium Kinetic Freeze-Out Properties in Relativistic Heavy-Ion Collisions from Energies Employed at the RHIC Beam Energy Scan to Those Available at the LHC. *Physical Review C*, 104, 034901. https://doi.org/10.1103/PhysRevC.104.034901